



RESEARCH ARTICLE

Determination of Cytotoxic and Apoptotic Properties of Lobaric Acid, a Secondary Metabolite of Lichen and Investigation of Its Theoretical Potential

Hamit Emre Kızıll¹ • Güleray Ağar² • Yavuz Ekincioglu¹ ¹Bayburt University, Vocational School of Health Services, Department of Medical Services and Techniques, Bayburt/Türkiye²Atatürk University, Faculty of Science, Department of Biology, Erzurum/Türkiye

ARTICLE INFO

Article History

Received: 22.07.2024

Accepted: 13.09.2024

First Published: 30.09.2024

Keywords

Apoptosis

Cytotoxicity

Lobaric acid

Molecular docking



ABSTRACT

In this study, we aimed to elucidate some of the mechanisms of cell death induced by lobaric acid in A549 (human lung cancer) cells. For this purpose, the effects of cytotoxic concentrations on p53 and caspase-3 gene expressions were investigated. A549 cells were treated with varying concentrations of lobaric acid (12.5, 25, 50, and 100 µg/ml) for 48 hours and then their viability was evaluated and p53 and caspase-3 mRNA expressions were determined at statistically cytotoxic concentrations of 12.5, 50, and 100 µg/ml. According to beta-actin, it was determined that the increase in lobaric acid concentration revealed an upward trend in p53 and caspase-3 mRNA expressions. Furthermore, quantum chemical parameters such as frontier molecular orbitals, band gap energy and ionization potential, electronic affinity, chemical softness, chemical potential, electrophilicity index and chemical hardness were analyzed. Furthermore, molecular docking was performed to identify the binding sites and the binding behavior of lobaric acid to some target proteins (P53, Caspase-3 and Bcl-2).

Please cite this paper as follows:

Kızıll, H. E., Ağar, G., & Ekincioglu, Y. (2024). Determination of cytotoxic and apoptotic properties of lobaric acid, a secondary metabolite of lichen and investigation of its theoretical potential. *Journal of Agricultural Production*, 5(3), 192-200. <https://doi.org/10.56430/japro.1518450>

1. Introduction

Health problems constitute an important part of the problems that arise in parallel with the continuous change in our world. The frequency and high mortality of cancer, one of the most important health problems of today, has caused the disease to become an important public health problem. The rate of spread of the first six types of cancer published by the International Agency for Research on Cancer in 2002 is as follows: lung, stomach, bladder, colorectal, laryngeal, larynx and prostate cancers in men, and breast, colorectal, stomach,

ovarian, lung and leukemia in women (Çakabay, 2012). Cancer is a multistep and multifactorial disease caused by hereditary and environmental factors. Somatic and inherited mutations, diet and environmental factors are considered to be the causes of cancer (Lichtenstein et al., 2000). For years, scientists have been making intensive efforts for the diagnosis and treatment of cancer, which is a multistep and multifactorial disease caused by hereditary and environmental factors. Studies have been conducted on molecular changes that are effective in the emergence of cancer stages, and alternative treatment methods

✉ Correspondence

E-mail address: ekizil@bayburt.edu.tr

and active substance applications have been used for centuries in the treatment of the disease (Takayama et al., 2006). The use of natural complementary and alternative products has become widespread due to the fact that chemotherapy and radiotherapy methods and surgical operations used in the treatment process of cancer do not show enough benefit (Emsen, 2015). The most remarkable group of organisms used in these studies are lichens. It is reported that more than 17000 species of lichens have been identified since the 18th century and more than 2000 species are found in North America. Initially believed to be a plant, lichens were later understood to be symbiotic organisms consisting of a fungal partner called a mycobiont and a photosynthetic partner called a photobiont, which may be one or more algae or cyanobacteria, as a result of studies by Schwender and Trebox (Aprile et al., 2011). Lichens are completely separate from the fungi and algae that make up their structure (Nash, 1996). Lobaric acid, secondary metabolites isolated from the Antarctic lichen *Stereocaulon alpinum*, is characterized by its significant bioactivity, demonstrating a range of pharmacological properties and represents a unique class of bioactive molecules with substantial potential for therapeutic applications (Seo et al., 2009). Moreover, these compounds have been demonstrated to exhibit a spectrum of biological activities, encompassing anti-proliferative, anti-inflammatory, antioxidant, and antimicrobial effects. Their therapeutic potential extends to a variety of pathological conditions, highlighting their multifaceted bioactivity and the promise they hold for future pharmacological development (Ögmundsdóttir et al., 1998). Lobaric acid was reported to have high antimycobacterial activity (Ingólfssdóttir et al., 1998). Moreover, in another study, it was shown that lobaric acid had antiproliferative and cytotoxic effects on breast cancer cells T-47D and ZR-75-1 and leukemia cells K-562 according to 5-lipoxygenase inhibitory activity (Ögmundsdóttir et al., 1998). The cytotoxic and antioxidative properties of lobaric, atranorin, salazinic, barbatic, α -alectoronic, α -collatolic, cryptochloroic, caperatic and protolicesterinic acid obtained from 6 lichen species collected from Brazil and Antarctica were determined and certain NMR and cytotoxicity profiles were established (Ravaglia et al., 2014). Morita et al. (2009) emphasized that lobaric acid has an inhibitory effect on tubulin polymerization (Morita et al., 2009). Thadhani et al. (2012) found that lobaric acid showed high antimicrobial activity against *Escherichia coli* bacteria (Thadhani et al., 2012). In another study, it was reported that lobaric acid and lecanoric acid showed very strong antioxidant properties (Thadhani et al., 2011). Based on the findings of these studies, in this study, the cytotoxic and apoptotic properties of lobaric acid in A549 (human lung cancer) cell line was determined and molecular docking studies were performed with p53, Caspase-3 and Bcl-2 proteins.

2. Materials and Methods

2.1. Cell Culture

To observe the cytotoxic and apoptotic effect of lobaric acid, A549 (human lung cancer) cell line was purchased from Santa Cruz Biotech (Heidelberg-Germany). Stock cells stored at -196 °C were removed and thawed. Cells were centrifuged at 2000 rpm and the filtrate was discarded and transferred into 25 ml flasks with 10% FBS (Biochrome AG). Passaging was performed for 24 - 48 hours in a light-free environment with 5% CO₂ (CO₂ Incubator Thermo). After transfer to larger flasks (Greiner), dead and waste cells were removed by washing with 8 ml PBS. In order for the flasks with a polylysine layer to release the cells, 2-3 ml trypsin was added and left for 2-3 min. After the cells in the flask were examined under inverted microscope, 3 ml of FBS was added to eliminate the toxic effect of trypsin and the cells were transferred to a falcon tube. After centrifugation at 2000 rpm for 5 min, the filtrate was discarded and up to 1 ml of DMEM (Gibco) was added to the tube. A mixture of 20 μ l of cells and 20 μ l of trypan blue (Sigma) was loaded into a hemocytometer and cell count was performed. After cell counting, 1x10⁶ cells/ml cells were transferred to each well of 96-well plates. This number was incubated for 24 hours to reach 2-fold and growth was observed under the microscope (Zeiss-Germany). Lobaric acid was first dissolved in 5 ml DMSO (Merck) + 995 ml DMEM. Then the concentrations of the substances were adjusted by serial dilution. Different concentrations of lichen acids were added to the cultured cells in triplicate except for the control group. 100 μ l of 10% FBS (9 ml DMEM 1 ml FBS) and 100 μ l of 10% DMSO were used as control groups (Kapuci et al., 2014).

2.2. Wst-1 Analysis

The 96-well microplate with a cell density of 2x10⁶ cells/ml, incubated in an incubator at 37 °C and 5% CO₂ for 24 hours, was removed from the incubator and the supernatants in the wells were removed. Lobaric acid was added to the wells at the determined concentrations (12.5, 25, 50, 100 μ g/ml) except for the negative control group. After 100 μ l of 10% FBS (9 ml DMEM 1ml FBS) was added to the control wells, they were kept in incubation for 48 hours to see the effect of the substance on the cells. After 48 hours, the cells taken from the incubation were examined morphologically under an inverted microscope and the optimum time period for application was determined. At this stage, the yellow WST-1 (Roche-Germany) dye turned into blue purple formazone as a result of the breakdown of the tetrazolium ring. After removal from incubation, absorbance values at 490/690 nm wavelength were calculated on a microplate reader (Bio-Tek Powervawe-Winooski). Cell viability was calculated using the following formula: Cell Viability = (Sample Absorbance / Control Absorbance) X 100 (Kapuci et al., 2014).

2.3. Gene Expression Analysis

In the initial phase of the experiment, total RNA was meticulously extracted from cells treated with lobaric acid using the Qiagen RNeasy mini kit (Qiagen, Germany), adhering to established protocols for optimal yield and purity. Following RNA isolation, the synthesis of complementary DNAs (cDNAs) was performed using the Qiagen RT2 First Strand cDNA synthesis kit (Qiagen, Germany), ensuring the accurate transcription of mRNA into stable cDNA for subsequent analysis. In the final analytical phase, the relative mRNA transcript levels of the genes encoding cysteine aspartate-specific protease-3 (caspase-3) and tumor protein p53 were quantitatively assessed through the RT-PCR technique. This process involved preparing a reaction mixture comprising gene-specific primers, synthesized cDNAs, and SyberGreen Master Mix (Qiagen, Germany), followed by initiation of the reaction in the ROTORGENEQ system (Qiagen, Germany). The data obtained from qRT-PCR were rigorously analyzed using the comparative threshold cycle (Ct) method, as described by Livak and Schmittgen (2001). ACTB was employed as an internal control to normalize the expression levels and ensure data accuracy.

2.4. Computational Study

Density functional theory (DFT) calculations were carried out using Gaussian 09 package software and Gaussian files were displayed using the molecular visualization application Gauss-View (Frisch et al., 2009). The optimized structural geometry of lobaric acid was determined utilizing the B3LYP functional and 6-311++G (d, p) basis set. The highest occupied molecular orbital (HOMO) and lowest unoccupied molecular orbital (LUMO) energy research was performed by the same level. The Auto-Dock Vina software (Trott & Olson, 2010) application was used to calculate the binding affinities and types of interactions between the ligand (lobaric acid) and target proteins. In addition, Discovery Studio software (Biovia, 2019) was utilized to view the ligand and protein's expected docking poses.

2.5. Statistical Analyzes

The experiment was carried out in triplicate, and the results are reported as the mean \pm standard deviation. Statistical analysis was conducted using SPSS 18.0 software, with a two-way analysis of variance (ANOVA). Duncan's multiple comparison test was applied to assess differences between the means, with a significance level of 5%.

3. Results and Discussion

3.1. Cytotoxicity Results

A549 cells were treated with 4 different concentrations of lobaric acid (12.5, 25, 50 and 100 $\mu\text{g/ml}$) for 48 hours and viability rates were determined (Table 1). Although all concentrations applied for treatment caused a decrease in viability rates, no concentration was found to be statistically significant ($p < 0.05$).

Table 1. Cell viability results of 48th hour lobaric acid treatment (SD \pm : standart deviation, % Viability: WST-1 assay results. Mean: the average of the test results performed in triplicate).

Concentrations	Mean \pm SD (% Viability)
Control	100 \pm 0
100 $\mu\text{g/ml}$	90.9 \pm 1.32
50 $\mu\text{g/ml}$	94.0 \pm 1.25
25 $\mu\text{g/ml}$	95.5 \pm 0.96
12.5 $\mu\text{g/ml}$	95.8 \pm 0.88

3.2. mRNA Expression Results

By using qRT-PCR, the expression profiles of the p53 and Caspase-3 genes in the A549 cells in the control and treatment groups were assessed. Since 25 and 12.5 $\mu\text{g/mL}$ concentrations were similar according to the cytotoxicity results, 100, 50 and 12.5 $\mu\text{g/mL}$ concentrations were used to determine mRNA expression levels. In the relative evaluation of both p53 and Caspase-3 mRNA expression levels compared to beta actin, it was determined that as the concentration increased, mRNA expression levels also increased. This means that the expression levels of apoptotic genes increased with lobaric acid treatment (Figure 1).

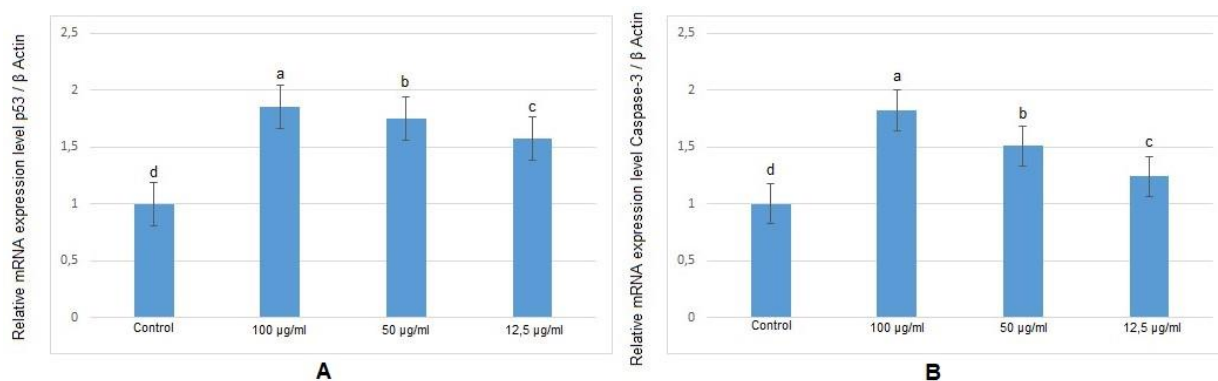


Figure 1. Effects of lobaric acid treatments on p53/Caspase-3 mRNA expression levels in A549 cells. (A) p53 mRNA transcript levels, (B) Caspase-3 mRNA transcript levels. Values are expressed as mean \pm SD. Different letters (a–d) on the columns show a statistical difference ($p < 0.05$).

3.3. Frontier Molecular Orbitals

Frontier Molecular Orbitals (FMOs) are utilized to study the reactive regions in molecular systems. Additionally, they determine the chemical reactivity of the molecules. FMOs are known as HOMO and LUMO. HOMO is the highest occupied molecular orbital and also an electron-rich orbital while LUMO is the lowest unoccupied molecular orbital and also an electron-poor orbital. These two molecular orbitals are very important for understanding quantum chemistry, biological processes, electrical and optical characteristics, and medicinal research (Ekincioglu, 2023; Srivastava, 2021). The energy difference between HOMO and LUMO orbitals is known as the band gap energy which indicates a molecule's stability and reactivity. If a molecule's band gap energy is large, it is more stable or has less chemical reactivity. The HOMO and LUMO molecular orbital distributions calculated are presented in Figure 2.

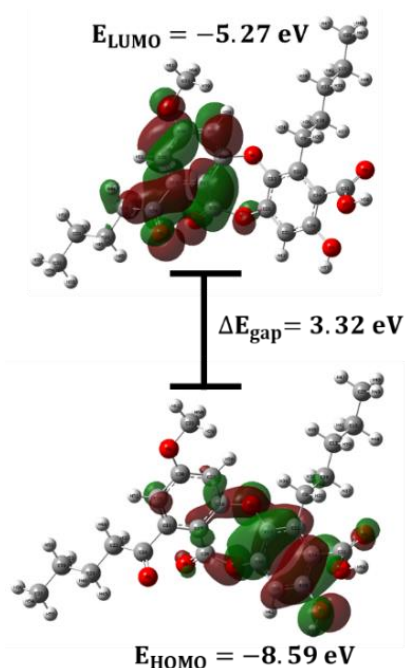


Figure 2. HOMO and LUMO patterns of lobaric acid.

FMOs analysis of the lobaric acid molecule showed that HOMO is located on the benzene ring region containing atoms C11 and C21, whereas LUMO is localized on the benzene ring region containing atoms C19 and C27. As a result of the calculations, the HOMO, LUMO, and band gap energy values were determined to be -8.59, -5.27, and 3.32 eV, respectively. Quantum chemical descriptors of a molecule can be determined utilizing FMOs, and they can be derived from Koopman's theorem which represents a theoretical method for connecting the chemical activities (ionization potential (IP), electronic affinity (EA), Chemical softness (S), Chemical potential (μ), electrophilicity index (ω) and chemical hardness (η)) of molecular structures to their electronic properties (Koopmans, 1934) and they may be utilized to study pharmacological characteristics and interactions with biological targets (González-González et al., 2023; Srivastava, 2021). The obtained quantum chemical descriptors values are presented Table 2. The quantum chemical descriptors parameters' mathematical definitions are as following equations:

$$IP = -E_{HOMO} \quad (1)$$

$$EA = -E_{LUMO} \quad (2)$$

$$S = \frac{1}{\eta} \quad (3)$$

$$\mu = -\frac{(IP+EA)}{2} \quad (4)$$

$$\omega = \frac{\mu^2}{2\eta} \quad (5)$$

$$\eta = \frac{(IP-EA)}{2} \quad (6)$$

Table 2. The HOMO, LUMO, Band gap energies and quantum chemical parameters.

Parameters	Values (eV)
E_{HOMO}	-8.59
E_{LUMO}	-5.27
Band gap energy (ΔE_{gap})	3.32
Ionization potential	8.59
Electron affinity	5.27
Chemical softness	0.60
Chemical potential	-6.93
Electrophilicity index	14.46
Chemical hardness	1.66

The IP and EA were calculated as 8.59 and 5.27 eV, respectively. The high IP values indicate a lower losing electron, whereas the high EA values indicate a greater accepting electron. The η and S of a molecule play a key role in defining its chemical reactions (Fahim & Farag, 2020). The obtained S and η values are 0.60 and 1.66 eV, respectively. To assess the chemical reactivity and bind to the molecule's biomolecules (Cárdenas et al., 2009; Mushtaq et al., 2024) the μ and ω values are essential. These values are obtained as -6.93 and 14.46 respectively. As a result, we can say that the molecule examined is hard and has good electrophilic behavior.

3.4. Molecular Docking

Molecular docking was used to investigate the binding mode, affinity, and potential interactions between P53, Caspase-3 and Bcl-2 genes and lobaric acid. The crystal structures of p53 (PDB: 6BSC), Caspase-3 (PDB: 3GJQ) and Bcl-2 (PDB:4MAN) were downloaded from the RCSB Protein Data Bank (<https://www.rcsb.org>) as the docking templates. We used Open Babel to get the ligand ready for docking (O'Boyle et al., 2011). We employed a docking approach that was previously reported (Ekincioğlu, 2023). For interaction between 6BSC (p53) and ligand, the coordinates for the center of the search space were -19.262, 11.658, and -4.339 Å along the x-, y-, and z-axis, respectively, for a cubic grid box with 90×90×90 Å sides. For interaction between 3GJQ (Caspase-3) and ligand, the coordinates for the center of the search space were 17.908, 14.402, and 17.76 Å along the x-, y-, and z-axis, respectively, for a cubic grid box with 90×90×90 Å sides. For interaction between 4MAN (Bcl-2) and ligand, the coordinates for the center of the search space were -12.102, -4.527, and -4.341 Å along the x-, y-, and z-axis, respectively, for a cubic grid box with 90×90×90 Å sides. Internal conformational search was conducted using the Lamarckian Genetic Algorithm. Hydrogen atoms and Kollman-type charges were added to the proteins by using AutoDock tools (Trott & Olson, 2010). Biovia discovery software was used to view the interactions between lobaric acid and proteins (Table 3) (Biovia, 2019).

Table 3. RMSD, Binding Energy and inhibition constant of different poses of Lobaric acid with 6BSC, 3GJQ and 4MAN as predicted by Auto dock Vina.

Mode	Lobaric acid and 6BSC			Lobaric acid and 3GJQ			Lobaric acid and 4MAN		
	RMDS	Binding Energy (kcal/mol)	Inhibition Constant (Ki) (mM)	RMDS	Binding Energy (kcal/mol)	Inhibition Constant (Ki) (mM)	RMDS	Binding Energy (kcal/mol)	Inhibition Constant (Ki) (mM)
1	34.73	-1.53	74.98	44.01	-1.50	79.29	21.41	-2.43	16.62
2	20.87	-1.50	80.17	43.47	-0.94	-	16.23	-1.69	57.96
3	30.05	-1.49	80.42	41.68	-1.29	113.22	24.08	-1.61	65.86
4	33.05	-1.31	109.08	35.52	-1.01	181.24	20.70	-1.59	68.28
5	30.76	-0.98	192.08	4023	-0.99	188.49	28.04	-1.34	104.99
6	21.39	-0.92	212.31	33.82	-0.80	259.11	19.62	-1.31	108.98
7	21.48	-0.81	254.89	37.79	-0.72	294.30	17.71	-1.25	120.35
8	36.22	-0.25	654.78	40.11	-0.56	386.52	15.07	-1.13	149.38
9	19.60	-0.13	800.13	38.38	-0.51	421.71	15.67	-0.74	288.13
10	26.36	-0.03	944.06	41.44	-0.40	509.60	19.96	-0.07	884.26

The obtained results between P53, Caspase-3 and Bcl-2 genes and lobaric acid are presented in Table 1 and Figure 3. We calculated root-mean-square deviation (RMSD), a commonly utilized measure of protein and ligand stability in complexes. The obtained results reveal that the RMDS values between proteins and ligand are 34.73, 44.01, and 21.41 for 6BSC, 3GJQ, and 4MAN, respectively. The binding affinities

obtained as a result of interaction for 6BSC, 3GJQ, and 4MAN are -1.53, -1.50 and -2.43 kcal/mol-1, respectively. The calculated inhibition constant values as a result of the interaction between proteins and ligand were 74.98 (6BSC), 79.29 (3GJQ,) and 16.62 (4MAN) mM. As a result, we can say that the best docking score is between 4MAN and lobaric acid.

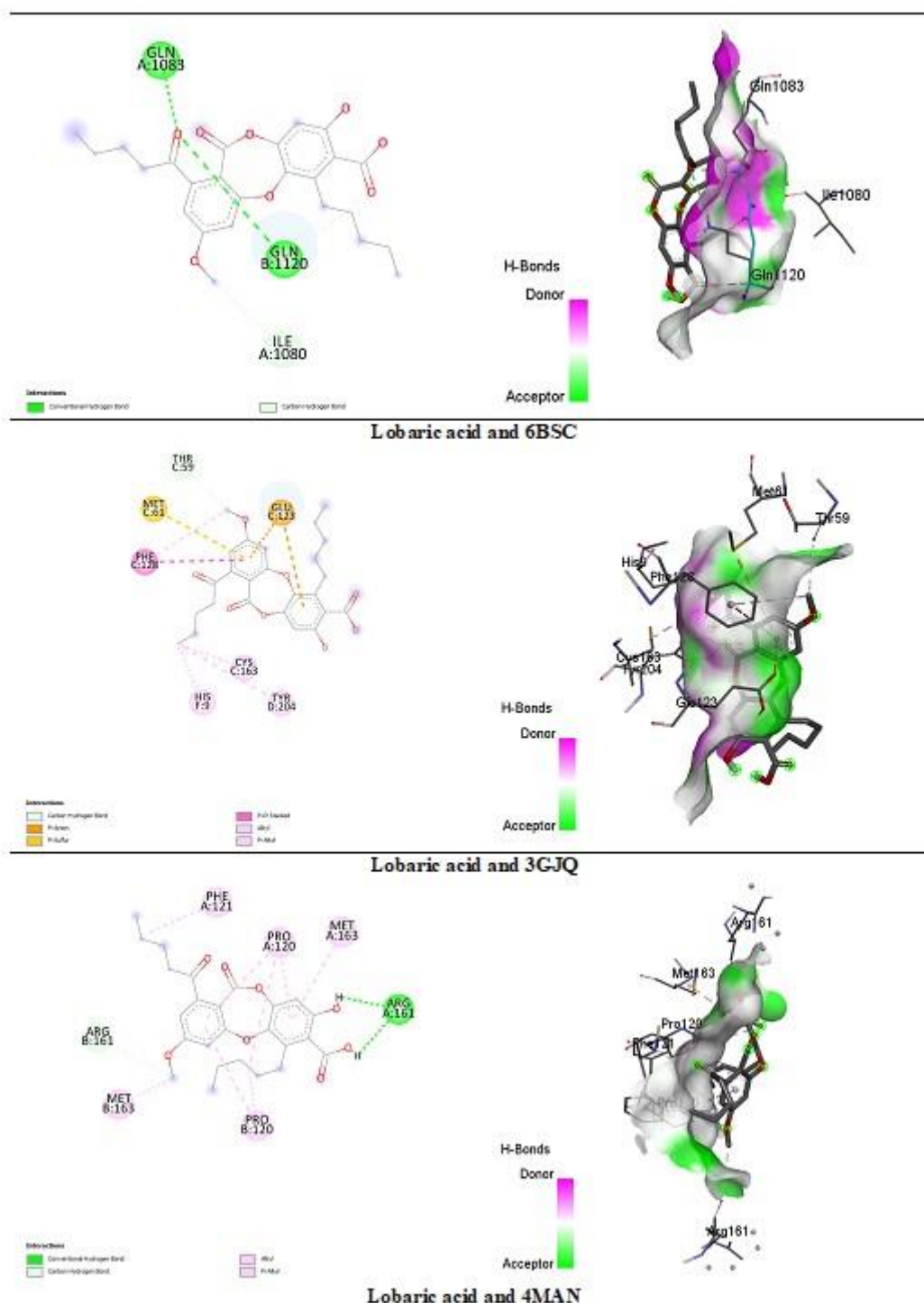


Figure 3. 2D molecular interaction and hydrogen binding surface of Lobaric acid with 6BSC, 3GJQ, and 4MAN.

The 2D molecular interaction and the hydrogen surface of lobaric acid with 6BSC, 3GJQ, and 4MAN is presented in figure 3. The active sites for 6BSC were determined as GLN 1083, GLN 1120, and ILE 1080, wherein green and light green balls represent conventional hydrogen bonds and carbon hydrogen bonds, respectively. The active sites for 3GJQ were found as GLU 123, MET 61, THR 59, PHE 128, CYS 163, HIS 9, and THR 204, wherein light green balls, gold balls, light gold balls, pink balls, and light pink balls represent carbon hydrogen

bonds, Pi-Anion, Pi-Sulphur, Pi-Pi stacked, alkyl, and Pi-alkyl interactions, respectively. The active sites for 4MAN were determined as ARG A: 161, ARG B: 161, PHE A: 121 PRO A-B:120, and MET A-B: 163, wherein green, light green balls, light pink balls, and light pink balls represent conventional hydrogen bond and carbon hydrogen bonds, alkyl and pi-alkyl interactions, respectively.

Lichens, a group of symbiotic organisms dating back 400 million years and different from plant species, have attracted researchers due to their ability to synthesize a high amount and variety of metabolites at once and their biological activities have been the subject of various studies for years (Spribille et al., 2022). Especially considering the inadequacy of various chemotherapeutics and radiotherapy agents used in cancer treatment studies and their failure to obtain a definite response to treatment, interest in lichens with antimicrobial, antitumoral, antifungal and antioxidant properties has increased and many successful studies have been carried out by using both lichen extracts and lichen active ingredients (Aydın, 2012; Çapık, 2014). Hong et al. (2018) assessed how lobaric acid and lobarstin affect human cervix adenocarcinoma HeLa cells and colon carcinoma HCT116 cells, demonstrating that treatment with these compounds significantly reduced the proliferation of both HeLa and HCT116 cells in a manner dependent on both dosage and duration. In another study conducted in the same year, Emsen et al. (2018) showed that LA was highly toxic on Glioblastoma multiforme (GBM) and primary rat cerebral cortex (PRCC) cells. In another study on lobaric acid, lobaric acid was found to have a high inhibitory effect on 12(S)-lipoxygenase platelets (Bucar et al., 2004). Andania et al. (2019) conducted a study highlighting the potent activity of the methanolic extract derived from *A. submutica* rhizomes against the MCF-7 breast adenocarcinoma cell line, achieving an IC50 value of 70.95 µg/mL. Their investigation further revealed that while most isolated compounds showed minimal effectiveness against both MCF-7 and HSC-3 cell lines, atranorin (1), lobaric acid (6), and methyl-β-orsinol carboxylate (9) exhibited notable anticancer properties. Specifically, atranorin displayed an IC50 value of 208.20 µM against MCF-7, while lobaric acid and methyl-β-orsinol carboxylate showed IC50 values of 172.05 µM and 382.60 µM, respectively, against the same cell line. In contrast, lobaric acid demonstrated an IC50 of 260.09 µM against HSC-3, whereas methyl-β-orsinol carboxylate exhibited a more potent effect with an IC50 of 88.92 µM. In our study, lobaric acid was found to reduce the cell viability of A549 cancer cells at concentrations of 12.5, 25, 50 and 100 µg/ml according to WST-1 results. Caspase-3 and p53 gene expressions of A549 cancer cells treated with lobaric acid also increased at concentrations of 12.5, 50 and 100 µg/ml. In addition, molecular docking of lobaric acid was investigated to give an insight of its activity against p53 (PDB: 6BSC), Caspase-3 (PDB: 3GJQ) and Bcl-2 (PDB:4MAN) were downloaded from the RCSB Protein Data Bank (<https://www.rcsb.org>) were investigated.

4. Conclusion

It is predicted that some concentrations of lobaric acid may show antiproliferative and apoptotic properties in A549 (human lung cancer) cell line. However, further molecular, cytological and in vivo studies are needed to determine the mechanism of

apoptosis and the antiproliferative and apoptotic properties of lobaric acid in more detail and to elucidate the mechanism of action. These results give a clue that cell death may occur apoptotically. However, examination of the mRNA expressions of many genes in the apoptotic pathway will lead us to a clearer conclusion. Quantum chemical calculation of lobaric acid were carried out using DFT/B3LYP/6-311++G(d,p) level of theory. The frontier molecular orbital research demonstrated that the energy HOMO and LUMO, respectively, was -8.59 eV and -5.27eV. The value of the Band gap energy (ΔE_{gap}) has been calculated to be 3.32 eV. Quantum chemical parameters reveal that the molecule examined is hard and has good electrophilic behavior. The findings of molecular docking work reveal that lobaric acid indicated the highest binding affinity to the 4MAN. moreover, the target with a higher binding energy is shown to have a lower inhibition constant. Despite all these data, the biological activity of lobaric acid needs to be investigated by testing different molecular pathways. In addition, *in vivo* studies will help to remove many obstacles to the use of the molecule as a pharmacological agent.

Compliance with Ethical Standards

The authors declare that this study does not require ethical committee approval or any legal permission. This study includes data obtained from a doctoral dissertation completed in 2016 (YÖK ID: 426087), and in line with the decisions taken by Ulakbim TR Dizin, Ethics Committee Permission is required for studies to be published since 2020. Other data obtained are web-based, virtual data.

Acknowledgment

Some of the data in this study were obtained from Dr. Hamit Emre KIZIL's PhD thesis (YÖK ID: 426087) completed in 2016. We are pleased to extend our deepest gratitude to the entire laboratory team for their unwavering moral support throughout the course of this doctoral thesis.

Conflict of Interest

The authors declare that they have no conflict of interest.

References

- Andania, M. M., Ismed, F., Taher, M., Ichwan, S. J. A., Bakhtiar, A., & Arbain, D. (2019). Cytotoxic activities of extracts and isolated compounds of some potential sumatran medicinal plants against MCF-7 and HSC-3 cell lines. *Journal of Mathematical & Fundamental Sciences*, 51(3), 225-242. <https://doi.org/10.5614/j.math.fund.sci.2019.51.3.2>
- Aprile, G., Catalano, I., Migliozi, A., & Mingo, A. (2011). Monitoring epiphytic lichen biodiversity to detect environmental quality and air pollution: The case study of Roccamonfina Park (Campania Region-Italy). In A.

- Moldoveanu (Ed.), *Air pollution-new developments* (pp. 227-245). IntechOpen. <https://doi.org/10.5772/17907>
- Aydın, S. (2012). *Elazığ yöresinde yetişen dut, kızcılık, kiraz ve ceviz meyvelerinin antioksidan kapasiteleri ve bazı deney modellerinde oluşturulan oksidatif stres üzerine etkilerinin incelenmesi* (Doctoral dissertation, Fırat University). (In Turkish)
- Biovia, D. S. (2019). *Discovery Studio Modeling Environment, Release 2017*. Dassault Systèmes.
- Bucar, F., Schneider, I., Ögmundsdóttir, H., & Ingólfssdóttir, K. (2004). Anti-proliferative lichen compounds with inhibitory activity on 12 (S)-HETE production in human platelets. *Phytomedicine*, 11(7-8), 602-606. <https://doi.org/10.1016/j.phymed.2004.03.004>
- Çakabay, B. (2012). *Meme kanserinde GASC1 ekspresyonu* (Specialty in medicine thesis, Ankara University). (In Turkish)
- Çapık, Ö. (2014). *Usnik asitin kültürü yapılmış huvec ve üç farklı kanser hücre hattı (A549, HeLa ve AGS) üzerine sitotoksik, antiproliferatif ve apoptotik etkisinin belirlenmesi* (Master's thesis, Atatürk University). (In Turkish)
- Cárdenas, C., Rabi, N., Ayers, P. W., Morell, C., Jaramillo, P., & Fuentealba, P. (2009). Chemical reactivity descriptors for ambiphilic reagents: Dual descriptor, local hypersoftness, and electrostatic potential. *The Journal of Physical Chemistry A*, 113(30), 8660-8667. <https://doi.org/10.1021/jp902792n>
- Ekincioglu, Y. (2023). Theoretical investigation of (E)-1-(2, 4-dichlorophenyl)-3-[4-(morpholin-4-yl) phenyl] prop-2-en-1-one molecule as a possible potential COVID-19 drug candidate: Molecular docking and DFT calculations. *Russian Journal of Physical Chemistry A*, 97(13), 3057-3067. <https://doi.org/10.1134/S0036024423130241>
- Emsen, B. (2015). *Liken sekonder metabolitlerinin deneysel beyin tümör modeli üzerine potansiyel etkilerinin in vitro yöntemlerle araştırılması* (Doctoral dissertation, Karamanoğlu Mehmetbey University). (In Turkish)
- Emsen, B., Aslan, A., Turkez, H., Taghizadehghaleh, J. A., & Kaya, A. (2018). The anti-cancer efficacies of diffractaic, lobaric, and usnic acid: In vitro: Inhibition of glioma. *Journal of Cancer Research and Therapeutics*, 14(5), 941-951. <https://doi.org/10.4103/0973-1482.177218>
- Fahim, A. M., & Farag, A. M. (2020). Synthesis, antimicrobial evaluation, molecular docking and theoretical calculations of novel pyrazolo [1, 5-a] pyrimidine derivatives. *Journal of Molecular Structure*, 1199, 127025. <https://doi.org/10.1016/j.molstruc.2019.127025>
- Frisch, M., Trucks, G., Schlegel, H. B., Scuseria, G. E., Robb, M. A., Cheeseman, J. R., Scalmani, G., Barone, V., Mennucci, B., & Petersson, G., & et al. (2009). *Gaussian 09, Revision B. 01*. Gaussian Inc.
- González-González, S., Franco-Pérez, M., Jardínez, C., Cariño-Moreno, J. J., Ramírez-Sotelo, M. G., & Zamudio-Medina, A. (2023). Synthesis, characterization, and quantum chemistry local chemical reactivity description of new phosphorylated derivatives of piperazine. *Phosphorus, Sulfur, and Silicon and the Related Elements*, 198(8), 693-703. <https://doi.org/10.1080/10426507.2023.2193404>
- Hong, J.-M., Suh, S.-S., Kim, T. K., Kim, J. E., Han, S. J., Youn, U. J., Yim, J. H., & Kim, I.-C. (2018). Anti-cancer activity of lobaric acid and lobarstin extracted from the antarctic lichen *Stereocaulon alpnum*. *Molecules*, 23(3), 658. <https://doi.org/10.3390/molecules23030658>
- Ingólfssdóttir, K., Chung, G. A., Skúlason, V. G., Gissurason, S. R., & Vilhelmsdóttir, M. (1998). Antimycobacterial activity of lichen metabolites in vitro. *European Journal of Pharmaceutical Sciences*, 6(2), 141-144. [https://doi.org/10.1016/S0928-0987\(97\)00078-X](https://doi.org/10.1016/S0928-0987(97)00078-X)
- Kapuci, M., Ulker, Z., Gurkan, S., & Alpsoy, L. (2014). Determination of cytotoxic and genotoxic effects of naphthalene, 1-naphthol and 2-naphthol on human lymphocyte culture. *Toxicology and Industrial Health*, 30(1), 82-89. <https://doi.org/10.1177/0748233712451772>
- Koopmans, T. (1934). Über die zuordnung von wellenfunktionen und eigenwerten zu den einzelnen elektronen eines atoms. *Physica*, 1(1-6), 104-113. [https://doi.org/10.1016/S0031-8914\(34\)90011-2](https://doi.org/10.1016/S0031-8914(34)90011-2) (In German)
- Lichtenstein, P., Holm, N. V., Verkasalo, P. K., Iliadou, A., Kaprio, J., Koskenvuo, M., Pukkala, E., Skytthe, A., & Hemminki, K. (2000). Environmental and heritable factors in the causation of cancer—analyses of cohorts of twins from Sweden, Denmark, and Finland. *The New England Journal of Medicine*, 343(2), 78-85. <https://doi.org/10.1056/NEJM200007133430201>
- Livak, K. J., & Schmittgen, T. D. (2001). Analysis of relative gene expression data using real-time quantitative PCR and the 2⁻ΔΔCT method. *Methods*, 25(4), 402-408. <https://doi.org/10.1006/meth.2001.1262>
- Morita, H., Tsuchiya, T., Kishibe, K., Noya, S., Shiro, M., & Hirasawa, Y. (2009). Antimitotic activity of lobaric acid and a new benzofuran, sakisacaulon A from *Stereocaulon sasakii*. *Bioorganic & Medicinal Chemistry Letters*, 19(13), 3679-3681. <https://doi.org/10.1016/j.bmcl.2009.03.170>
- Mushtaq, A., Asif, R., Humayun, W. A., & Naseer, M. M. (2024). Novel isatin-triazole based thiosemicarbazones as potential anticancer agents: Synthesis, DFT and molecular docking studies. *RSC Advances*, 14(20), 14051-14067. <https://doi.org/10.1039/D4RA01937G>

- Nash, T. H. (1996). *Lichen biology*. Cambridge University Press.
- O'Boyle, N. M., Banck, M., James, C. A., Morley, C., Vandermeersch, T., & Hutchison, G. R. (2011). Open Babel: An open chemical toolbox. *Journal of Cheminformatics*, 3, 1-14. <https://doi.org/10.1186/1758-2946-3-33>
- Ögmundsdóttir, H. M., Zoëga, G. M., Gissurarson, S. R., & Ingólfssdóttir, K. (1998). Natural products: Anti-proliferative effects of lichen-derived inhibitors of 5-lipoxygenase on malignant cell-lines and mitogen-stimulated lymphocytes. *Journal of Pharmacy and Pharmacology*, 50(1), 107-115. <https://doi.org/10.1111/j.2042-7158.1998.tb03312.x>
- Ravaglia, L. M., Gonçalves, K., Oyama, N. M., Coelho, R. G., Spielmann, A. A., & Honda, N. K. (2014). In vitro radical-scavenging activity, toxicity against *A. salina*, and NMR profiles of extracts of lichens collected from Brazil and Antarctica. *Química Nova*, 37, 1015-1021. <https://doi.org/10.5935/0100-4042.20140159>
- Seo, C., Sohn, J. H., Ahn, J. S., Yim, J. H., Lee, H. K., & Oh, H. (2009). Protein tyrosine phosphatase 1B inhibitory effects of depsidone and pseudodepsidone metabolites from the Antarctic lichen *Stereocaulon alpinum*. *Bioorganic & Medicinal Chemistry Letters*, 19(10), 2801-2803. <https://doi.org/10.1016/j.bmcl.2009.03.108>
- Spribille, T., Resl, P., Stanton, D. E., & Tagirdzhanova, G. (2022). Evolutionary biology of lichen symbioses. *New Phytologist*, 234(5), 1566-1582. <https://doi.org/10.1111/nph.18048>
- Srivastava, R. (2021). Theoretical studies on the molecular properties, toxicity, and biological efficacy of 21 new chemical entities. *ACS Omega*, 6(38), 24891-24901. <https://doi.org/10.1021/acsomega.1c03736>
- Takayama, T., Miyanishi, K., Hayashi, T., Sato, Y., & Niitsu, Y. (2006). Colorectal cancer: Genetics of development and metastasis. *Journal of Gastroenterology*, 41, 185-192. <https://doi.org/10.1007/s00535-006-1801-6>
- Thadhani, V. M., Choudhary, M. I., Ali, S., Omar, I., Siddique, H., & Karunaratne, V. (2011). Antioxidant activity of some lichen metabolites. *Natural Product Research*, 25(19), 1827-1837. <https://doi.org/10.1080/14786419.2010.529546>
- Thadhani, V. M., Choudhary, M. I., Khan, S., & Karunaratne, V. (2012). Antimicrobial and toxicological activities of some depsides and depsidones. *Journal of the National Science Foundation of Sri Lanka*, 40(1), 43-48. <https://doi.org/10.4038/jnsf.v40i1.4167>
- Trott, O., & Olson, A. J. (2010). AutoDock Vina: Improving the speed and accuracy of docking with a new scoring function, efficient optimization, and multithreading. *Journal of Computational Chemistry*, 31(2), 455-461. <https://doi.org/10.1002/jcc.21334>